1 The FSB Concept

We are developing a new technique for low noise sub-millimeter to mid-infrared sensing using a cryogenic bolometric detector as an active element in a tuned quasi-optical resonant interference filter. All filter and bolometer components are assembled from micromachined silicon structures. The absorption, transmission, and reflection characteristics of the detector depend on frequency in a controlled manner: a Frequency Selective Bolometer (FSB).

A set of FSBs will be cascaded within a straight light-guide to produce a high-efficiency, compact, multi-band radiometer. Instruments based on FSB technology will have important advantages over current multi-channel bolometric radiometers, including: 1) the expected coupling efficiency is several times higher than traditional multi-channel bolometer systems, significantly improving detector sensitivity; 2) the cryogenic optics are smaller and more compact, reducing the demands on cryostat size and weight; and 3) there is no restriction on the geometry in the focal plane. An FSB system is amenable to configuration as a close packed focal-plane array, permitting efficient use of the throughput of a telescope. These advantages are key for future sub-orbital, and space-based astrophysics and space-physics experiments.

In the near future, we plan to extend this design for use in the mid-infrared where compact, multi-frequency, high efficiency radiometers are important for airborne measurements.

2 Advantages of FSBs

Traditionally, multi-mode bolometric radiometers have used spectral filters to define the band of sensitivity and a broadband absorber, sometimes matched with a tuned backshort. . A number of such filters can be combined with several detectors to provide a multi-band dichroic system.

Alternatives to this type of system is either a filter wheel approach which requires sequential measurements to obtain spectral information, or a focal plane with different pixels having different spectral response.

The FSB system overcomes the limitations of these systems. Because it permits the possibility of cascading multiple FSBs within a straight light-pipe it enables a complete multi-channel radiometer in a single compact

cylinder. Arrays of such cylinders allow greater freedom in the geometry of the focal plane. Because of the small size of the FSB radiometer, the cryogenic system can be simplified. This has important benefits for space, airborne, and balloon-borne applications.

3 Figures and Tables

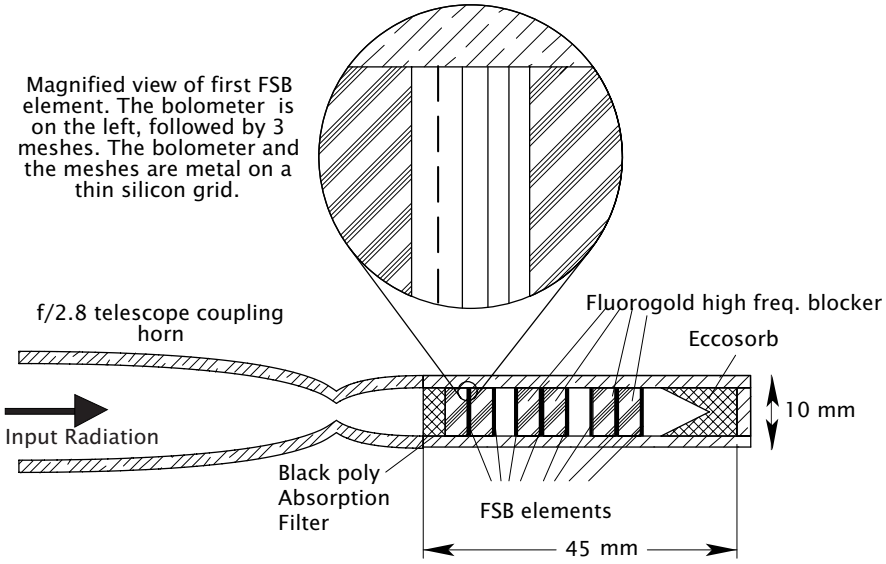

Figure 1: Schematic of a Frequency Selective Bolometer (FSB) Radiometer with eight frequency bands. The radiation enters the feed horn on the left. After passing through the étendu (0.15 cm^2 sr) defining aperture, the beam is expanded and passes through the FSB elements. Because each element absorbs only in a narrow range of frequencies, they can be cascaded. To avoid frequencies in the diffractive region of a given filter, the elements are arranged from highest to lowest frequency. Between FSBs, a high frequency absorber such as Fluorogold of the appropriate thickness reduces radiation above the design frequency. This example of an FSB radiometer, which we propose to construct and characterize is designed for the sub-millimeter. A similar, smaller device will be designed for use in the mid-infrared.

Kowitt, *et al.* 1996, Applied Optics

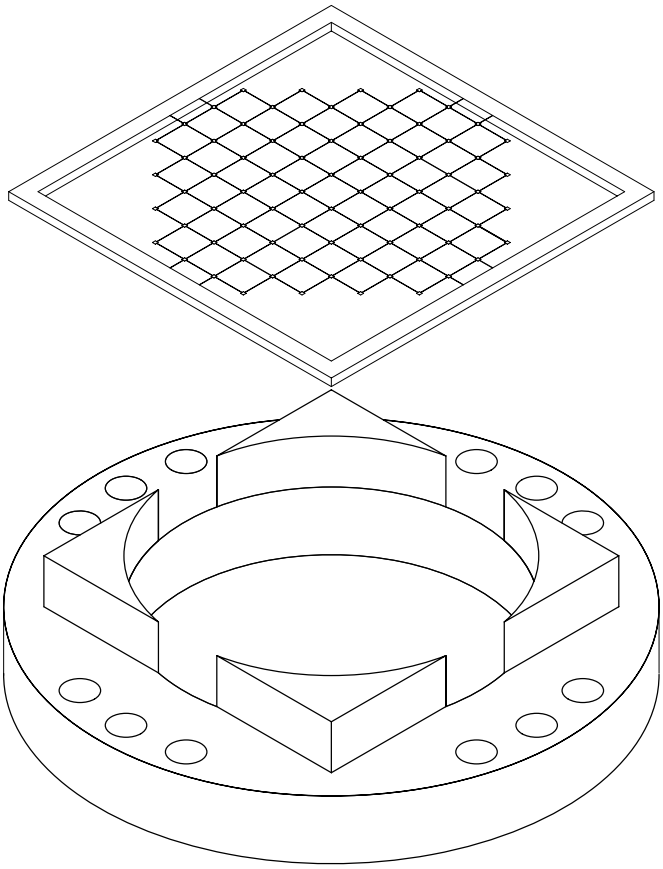

Figure 2: Drawing of a mesh on the silicon grid and the FSB mount. The mesh has a silicon frame by which the silicon grid is supported. The resonant metal mesh is in the silicon but is not visible in this drawing. The bolometer element will look identical to the meshes but the metalization thickness will be optimized for maximum absorption in band. The Invar mount is shown below the mesh for clarity. The holes in the mount are used to feed the leads from the up-stream FSB elements to the back.

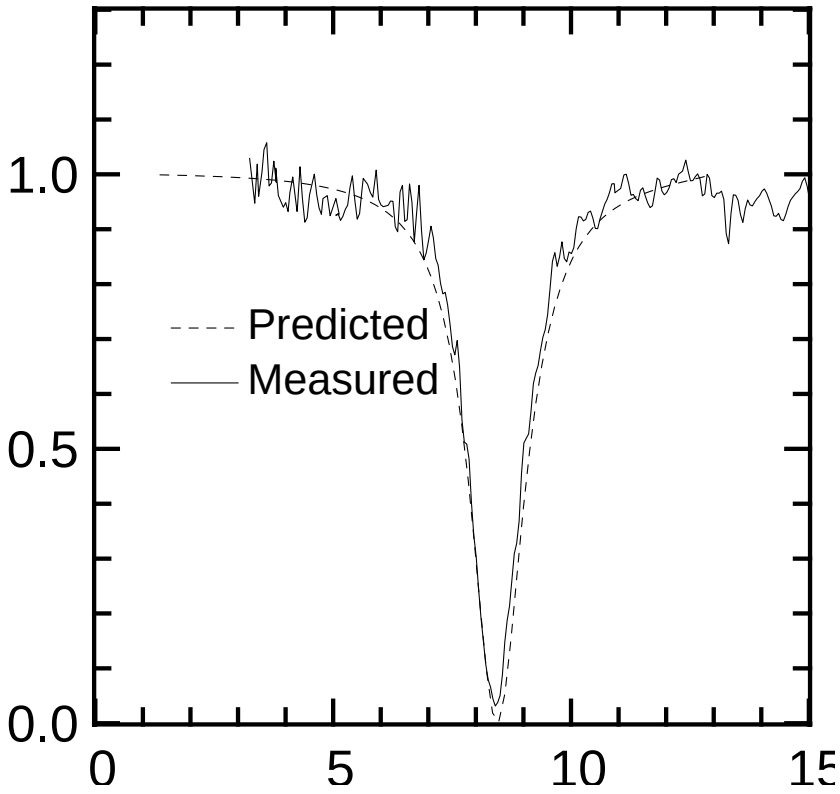

Figure 3: Comparison of analytic prediction and measurement of the transmission of a mesh of crosses on a silicon grid as shown in Fig. 2. In this case, the metalization has high conductivity and no losses. The measurement is made with an FTS interferometer with an étendu of 0.5 cm^2 sr on a full sized 1 cm diameter mesh. Detector noise causes the wiggles on the measurement line. An empirical shift of 15% due to the effects of the dielectric constant of the silicon grid has been fit in the mesh model.

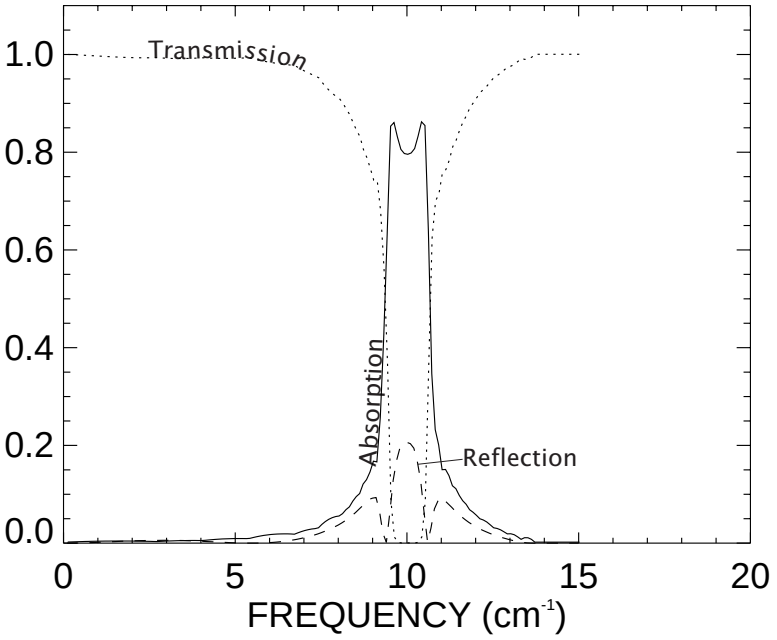

Figure 4: Modeled performance of an FSB element. The curves show the transmission, reflection, and absorption for the FSB versus frequency for a device tuned to $\nu_0 = 10$ cm^{-1}. High efficiency is possible for both absorption and transmission.

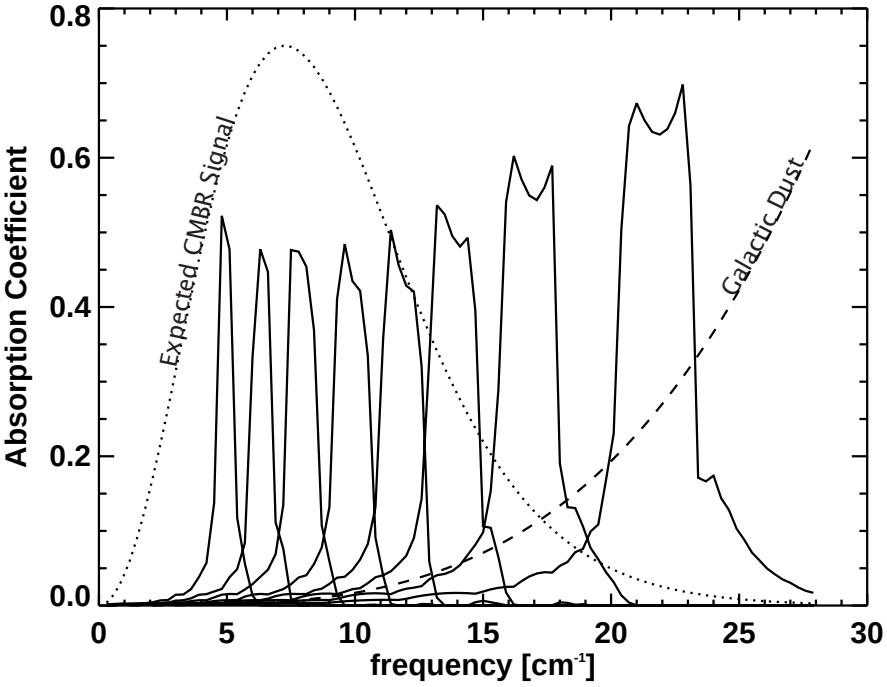

Figure 5: The model of the absolute absorption coefficient of an eight-band FSB system as a function of frequency. The detector geometry would be a small tube like that shown in Fig. 1. The calculations include the bolometer coupling efficiency and the losses in the high-frequency absorber material. Efficiency of typical dichroic, multi-spectral bolometers systems is less than 10%. These curves can be used to calculate the sensitivity of the system to a given signal. An example of such a calculation is shown in Table 1.

Projected FSB Based CMB Experiment Sensitivity

Model[d]	MSAM 1[a]	FSB[b]	Mapping Experiments[c]		
			FIRS[e]	*COBE*[f]	*combined*
	(μK RMS)	(μK RMS)	(μK RMS)	(μK RMS)	(μK RMS)
CMBR	21.	5.6	100.	80.	62.
CMBR+Dust$_1$	22.	5.6	120.	82.	67.
CMBR+Dust$_2$	35.	7.8	210.	180.	82.
CMBR+Dust$_1$+Brem	240.	38.	1500.	140.	95.
CMBR+Dust$_2$+Brem	240.[g]	38.	2600.[g]	360.	130.
CMBR+Dust$_1$+Brem+Sync	300.[g]	39.	4300.[g]	360.	170.

[a] Sensitivity per single difference, integrated for 10^3 seconds. Based on 20-minute integrated noise measured during June 1992 flight of MSAM 1.

[b] Sensitivity, single difference, integrated for 20 seconds. Based on Fig. 5, the bolometer model of Mather and a 0.3K cryostat.

[c] Sensitivity per 2°.5 pixel.

[d] Components are CMBR anisotropy, one- or two-parameter dust, bremsstrahlung, and synchrotron emission.

[e] Based on noise measured during October 1988 flight.

[f] Based on the DMR first-year map sensitivity. FIRAS sensitivity determines dust removal.

[g] No extra spectral degrees of freedom—simple solution only.

Table 1: A comparison of the modeled sensitivities of several experiments to the CMBR in the presence various sources of foreground emission with known spectrum but unknown amplitude. The figures are the RMS sensitivity per sky pixel in a given the integration time. For existing experiments, the figures are derived from achieved levels of sensitivity. For a single pixel FSB radiometer the RMS sensitivity is given for 20 seconds of integration. The first row of figures is the sensitivity of the experiment if no foreground removal is needed.